Effect of local magnetic moments on spectral properties and resistivity near interaction- and doping-induced Mott transitions

T. B. Mazitov [1] and A. A. Katanin [1,2]

[1] *Center for Photonics and 2D Materials, Moscow Institute of Physics and Technology, Institutsky Lane 9, Dolgoprudny, 141700 Moscow Region, Russia*

[2] *M. N. Mikheev Institute of Metal Physics, Kovalevskaya Street 18, 620219 Ekaterinburg, Russia*

(Received 5 August 2022; revised 14 November 2022; accepted 15 November 2022; published 28 November 2022)

We study the effect of the formation and screening of local magnetic moments on the temperature and interaction dependences of spectral functions and resistivity in the vicinity of the metal-insulator transition. We use dynamical mean-field theory for the strongly correlated Hubbard model and associate the peculiarities of the above-mentioned properties with those found for the local charge χ_c and spin χ_s susceptibilities. We show that at half filling the maximum of resistivity at a certain temperature T^* corresponds to the appearance of a central quasiparticle peak of the spectral function and entering the metallic regime with well-defined fermionic quasiparticles. At the same time, the temperature of the crossover to the regime with screening of local magnetic moments, determined by the minimum of double occupation, is smaller than the temperature scale T^* and coincides at half filling with the boundary $T_{\beta=1}(U)$ corresponding to the exponent of resistivity $\beta \equiv d\ln\rho/d\ln T = 1$. Away from half filling we find a weak increase of the temperature of the beginning and completion of the screening (i.e., Kondo temperature) of local magnetic moments, while the unscreened local magnetic moments exist only up to a few percent of doping. In the low-temperature regime $T < T_{\beta=1}$ the simultaneous presence of itinerant and localized degrees of freedom yields an almost linear temperature dependence of the scattering rate and resistivity.

DOI: 10.1103/PhysRevB.106.205148

I. INTRODUCTION

The Mott metal-insulator transition (MIT) [1] represents a phenomenon which occurs due to strong electronic correlations. It is observed in particular in transition metal oxides such as V_2O_3 [2–8], layered organic compounds [9–15], high-temperature cuprate superconductors (see, e.g., Ref. [16]), etc. The proximity to the Mott transition yields peculiarities of many physical properties, which can be related to the appearance of local magnetic moments (see, e.g., the discussion in Refs. [17–19]).

Quantitative studies of the Mott transition became possible with the discovery of the dynamical mean-field theory (DMFT) [20]. Originally, the Mott transition was described mainly on the basis of single-particle properties, e.g., spectral functions, densities of states, etc. [20]. The peculiarities of transport properties near the Mott transition were investigated in Refs. [21–29]. In this respect, the boundary of the metallic behavior (the so-called Brinkmann-Rice boundary), which can be determined from the maximum of the temperature dependence of resistivity, was introduced [13–15]. At the same time, the crossover between different states near the first-order transition can be characterized by the Widom line, which was first introduced in the context of the liquid-gas transition [30,31] as the line of a sharp change from a liquid to gaslike behavior above the critical temperature. For correlated electronic systems this boundary, corresponding to a sharp change from metal to insulating behavior, can be determined in particular from the inflection points of the resistivity $\rho(U)$ dependences [10,26], double occupation, or single-particle properties [29]. The relation of the Widom line to the second derivative of the Landau functional, determined by the convergence rate of DMFT solutions, was emphasized in Refs. [25,26]. Moreover, it was shown that near the Mott transition the interaction dependence of the resistivity [25–28], the spectral functions, and the self-energies [28] obey certain scaling laws, showing quantum critical behavior of these quantities.

Recently, in connection with the studies of the two-particle quantities near the Mott transition, the formation of local magnetic moments (LMMs) in the vicinity of the Mott transition [32–34] and the explicit determination of the Landau functional and its derivatives in terms of the local vertices [35] were discussed at half filling. In particular, criteria for determining the temperatures of the formation [33,34], start of screening [34], and fully screened (Kondo temperature) [32–34] local magnetic moments based on the peculiarities of the local charge and spin susceptibilities were proposed. The relation of these criteria to the above-mentioned features of the quantum critical behavior of resistivity near the Mott transition is, however, not obvious since it involves the relation of single-particle, local two-particle, and transport properties. Although at the level of DMFT for the single-band model the vertex corrections to transport properties vanish and the two-particle properties are not directly related to transport

properties, they are both related to the single-particle properties.

The resistivity at finite doping was studied previously within DMFT and cluster theories in Refs. [22,27,36]. While close to half filling the temperature dependence of the resistivity shows a maximum, which is similar to that for the half-filled case, the temperature interval of the pronounced almost linear temperature dependence of resistivity is obtained in this case. Again, the question of the connection between this behavior and peculiarities of single-particle quantities can be raised in this case.

In the present paper we study the connection between the above-described features of resistivity and the local single- and two-particle properties. In particular, we supplement a previous study of the formation of local magnetic moments at half filling [34] with a detailed study of the temperature and interaction dependence of resistivity within the Hubbard model on the square lattice. By comparing the obtained characteristic temperatures at half filling we find that different criteria for the Widom line T^* almost coincide with each other and with the start of the formation of quasiparticles. We also find the coincidence of the line of the resistivity exponent $\beta \equiv d\ln\rho/d\ln T = 1$ with the boundary of the start of the screening of local magnetic moments, determined previously from the minimum of local charge compressibility and double occupation. This provides a natural definition of this boundary in terms of directly measurable quantities and allows us to conclude that the temperature of screening of LMMs is located below T^*. Away from half filling we show the presence of screened LMMs. The boundary of the screening regime is determined by the minimum of double occupation, while the minimum of local charge compressibility disappears at sufficiently large doping due to the presence of free charge carriers. We also show that the exponent of the resistivity $\beta = 1$ corresponds to the onset of the linear temperature dependence of resistivity and quasiparticle damping in this case.

The plan of this paper is as follows. In Sec. II we briefly discuss the model and method, in Sec. III we present the results for half filling ($n = 1$; Sec. III A) and away from half filling ($n < 1$; Sec. III B). In Sec. IV we present conclusions.

II. THE MODEL AND METHOD

We consider the Hubbard model on a square lattice,

$$H = -t\sum_{\langle i,j\rangle,\sigma} c^\dagger_{i\sigma}c_{j\sigma} + U\sum_i n_{i\uparrow}n_{i\downarrow}, \tag{1}$$

and use the half bandwidth $D = 4t = 1$ as the unit of energy.

We apply the DMFT approach [20] and evaluate the self-energies $\Sigma(\nu)$ and respective local spectral functions $A(\nu)$ at the real frequency axis using the numerical renormalization group approach [37] within the TRIQS-NRG LJUBLJANA INTERFACE package [38]. Using DMFT results, we evaluate the conductivity starting with the Kubo formula

$$\sigma(i\omega_n) = \frac{2e^2T}{\omega_n}\sum_{\mathbf{k},\nu_n} v^2_{\mathbf{k},a}G(\epsilon_\mathbf{k}, i\nu_n)G(\epsilon_\mathbf{k}, i\nu_n + i\omega_n), \tag{2}$$

where $G(\epsilon, i\nu_n) = 1/[i\nu_n - \epsilon - \Sigma(i\nu_n)]$ are the Green's functions, $\epsilon_\mathbf{k} = -(\cos k_x + \cos k_y)/2$ is the dispersion, $v_\mathbf{k} = \nabla\epsilon_\mathbf{k} = (\sin k_x, \sin k_y)/2$ is the electron velocity, ν_n and ω_n are the fermionic and bosonic Matsubara frequencies, the factor of 2 comes from the spin summation, and we neglect the vertex corrections, which vanish in the DMFT for the single-band model. Introducing the partial density of states

$$\begin{aligned}\mathcal{D}_0(\epsilon) &= 2\sum_\mathbf{k}\sin^2 k_x\delta(\epsilon - \epsilon_\mathbf{k})\\ &= \frac{8}{\pi^2}[E(1-\epsilon^2) - \epsilon^2K(1-\epsilon^2)],\end{aligned} \tag{3}$$

where $E(x)$ and $K(x)$ are the complete elliptic integrals of the first and second kind, we find

$$\sigma(i\omega_n) = \frac{e^2T}{4\omega_n}\sum_{\nu_n}\int_{-1}^{1} d\epsilon\mathcal{D}_0(\epsilon)G(\epsilon, i\nu_n)G(\epsilon, i\nu_n + i\omega_n). \tag{4}$$

Using the spectral representation, performing the summation over Matsubara frequencies and analytic continuation to the real axis $i\omega_n \to \omega + i\delta$, and taking the real part of the limit $\sigma(\omega \to 0)$, we finally obtain the static conductivity

$$\sigma = -\frac{\pi e^2}{4}\int_{-1}^{1} d\epsilon\mathcal{D}_0(\epsilon)\int_{-\infty}^{+\infty} d\nu f'(\nu)A(\epsilon, \nu)^2, \tag{5}$$

where $A(\epsilon, \nu) = -(1/\pi)\mathrm{Im}G(\epsilon, \nu)$ is the spectral density. The position of the Widom line of the crossover from an incoherent metal to an insulating regime is determined from the maxima of the $\rho(T)$ dependence [13–15] or inflection points of the $\ln\rho(U)$ dependence [10,26]; we show below that these two criteria agree well with each other.

We are interested in the temperature range $T > T_K$, where T_K is the Kondo temperature of screening of local magnetic moments [22,34,39]. Therefore, the van Hove singularity of the density of states is cut by the temperature and quasiparticle damping, and we expect the obtained results to be not specific for the two-dimensional square lattice but qualitatively applicable for the other forms of the bare density of states not gapped at the Fermi level (see, e.g., the discussion in Ref. [40]).

At half filling, we also compare the position of the obtained Widom line to that found from the minimum of the lowest eigenvalue of the second derivative of the Landau functional Ω [35],

$$\frac{\delta^2\Omega}{\delta(i\Delta_\nu)\delta(i\Delta_{\nu'})} = \frac{\hat{1}}{\hat{1} - \hat{x}^{-1}\hat{X}}(\hat{1} - \hat{\mathcal{D}})\hat{x}, \tag{6}$$

where Δ_ν is the hybridization function of the impurity problem; $\mathcal{D}_{\nu\nu'} = (x_\nu - X_\nu)F^{\mathrm{loc}}_{\omega=0,\nu\nu'}$; $\hat{X}_\nu = -\hat{1}T\sum_\mathbf{k}G(\epsilon_\mathbf{k}, \nu)^2$ and $\hat{x}_\nu = -\hat{1}TG^2_{\mathrm{loc}}(\nu)$ are the nonlocal and local bubbles, considered to be diagonal in frequency operators ($\hat{1} = \delta_{\nu\nu'}$); $G_{\mathrm{loc}}(\nu)$ is the local Green's function; and $F^{\mathrm{loc}}_{\omega=0,\nu\nu'}$ is the zero bosonic frequency local vertex. The local vertices are evaluated by using the continuous-time quantum Monte Carlo impurity solver, implemented in the IQIST software package [41].

III. RESULTS

A. Half filling $n = 1$

We consider first the peculiarities of the resistivity near the Mott transition at half filling. The temperature dependence of the resistivity, calculated according to Eq. (5) for various values of the Coulomb interaction, is shown in Fig. 1(a). In agreement with previous studies on the infinite-dimensional hypercubic [21–23] and square [24] lattices, the obtained dependences show a maximum at some characteristic temperature $T^*(U)$, which decreases with an increase of the interaction strength. It was suggested (see also experimental studies of layered organic compounds [13–15]) that the maximum of the dependence $\rho(T)$ is related to the loss of quasiparticles with increasing temperature.

To confirm the relation of the obtained maxima of the resistivity to the loss of fermionic quasiparticles, we consider the temperature evolution of the electronic self-energy. Figure 1(b) shows the temperature dependences of $\mathrm{Im}\Sigma(\nu = 0)$ at various interaction strengths. Closed (open) circles correspond to the negative (positive) derivative $\partial \mathrm{Re}\Sigma(\nu)/\partial\nu$ and minimum (maximum) of $|\mathrm{Im}\Sigma(\nu)|$ at $\nu = 0$, corresponding to well-defined (destroyed) fermionic quasiparticles. As one can see, the change in the sign of the derivative occurs indeed at approximately the same temperatures as obtained from the maxima of the resistivity. We also compared the obtained temperature T^* to that of the change in the frequency dependence of the local spectral function $A(\nu) = -\mathrm{Im}G_{\mathrm{loc}}(\nu)/\pi$ [34]. We found that the appearance of the central quasiparticle peak of $A(\nu)$ also occurs at approximately the same temperature T^* as the maximum of the resistivity and onset of the quasiparticle shape of the electronic self-energy (this correspondence holds also for the other values of U; see below).

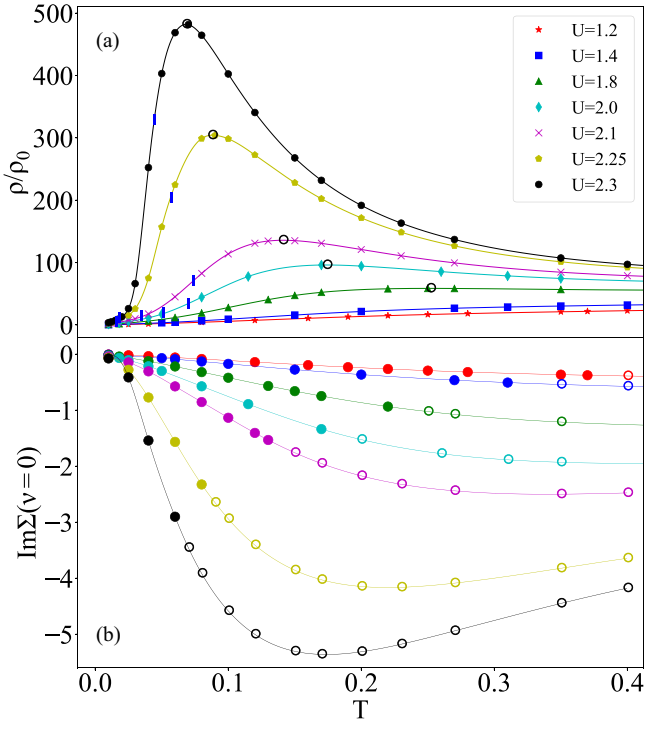

FIG. 1. Temperature dependences of (a) the resistivity [in units of $\rho_0 = \hbar/(4e^2)$] and (b) the imaginary part of zero-frequency self-energy at various values of U. The black open circles in (a) indicate maxima of ρ, and the blue bars in (a) indicate points where $\beta = d\ln\rho/d\ln T = 1$. Solid (open) circles in (b) indicate a negative (positive) sign of $\partial \mathrm{Re}\Sigma(\nu)/\partial\nu$.

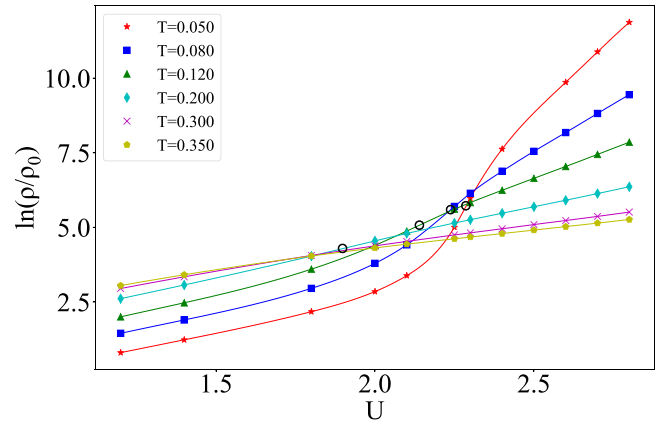

FIG. 2. Interaction dependence of the resistivity in logarithmic scale. The open circles indicate inflection points of the $\ln\rho(U)$.

The damping of the quasiparticles $\Gamma = -\mathrm{Im}\Sigma(0)$ at intermediate temperatures increases with increasing U and at the temperatures $T \sim T^*$ follows the linear temperature dependence $\Gamma \simeq \Gamma_0 + AT$ instead of the quadratic one for the Fermi liquid. We note that recently, similar linear temperature dependences of the quasiparticle damping were obtained in the combination of *ab initio* and DMFT studies of vanadium in the regime of partly formed local magnetic moments [42], although in the latter case it is caused by Hund's interaction instead of the proximity to the Mott insulator.

To determine the position of the Widom line from the resistivity, following Refs. [10,26], we also determine flection points of the $\ln\rho(U)$ dependences (see Fig. 2). We find that the flection points coincide to good accuracy with the above-discussed positions of maxima of $\rho(T)$ dependences, showing the uniqueness of determining the crossover from metallic to insulating phase near the Mott transition. Notably, the obtained dependences $\ln\rho(U)$ closely resemble the experimental data from Ref. [10] for the pressure dependence $\ln\rho(p)$ in the organic layered compound κ-$(\mathrm{ET})_2\mathrm{Cu}_2(\mathrm{CN})_3$.

The obtained results for the dependence of characteristic temperatures on the interaction strength are combined in Fig. 3 with previous results from Ref. [34] for characteristic temperatures obtained from the local charge and spin susceptibilities. We use the notations introduced in Ref. [34]: PLM stands for the preformed local moment regime, SCR is the regime of the local moment screening, and FL denotes the Fermi liquid state. As mentioned above, the temperatures T^* of the maxima of resistivity and appearance of quasiparticles in both the self-energy and local spectral functions almost coincide and mark the boundary of the quasiparticle (metallic) regime, which we denote by QP. The Widom line obtained from inflection points of $\ln\rho(U)$ also appears to be close to $T^*(U)$. We also note that the minima of the second derivative of the Landau functional are sufficiently close to the considered boundary, although they do not coincide with it precisely.

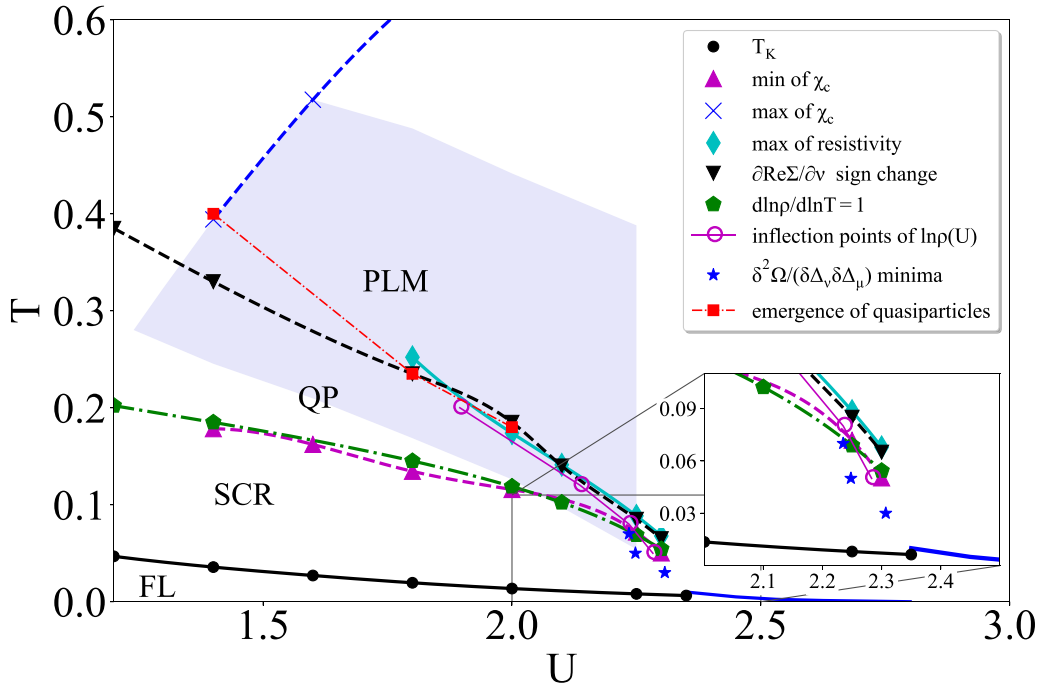

FIG. 3. The obtained phase diagram at $n = 1$. The turquoise line (rhombs) shows maxima of $\rho(T)$, and the green dash-dotted line (pentagons) indicates points corresponding to the exponent $\beta \equiv d\ln\rho/d\ln T = 1$. The temperatures for the appearance of quasiparticles obtained from the change in the sign of $\partial \mathrm{Re}\Sigma(\nu)/\partial\nu$ are shown by the black dashed line (triangles), and those obtained from the appearance of the peak of the spectral function are shown by the red dashed line (squares). The Widom line determined from the inflection points of $\ln\rho(U)$ is shown by the purple line (open circles), and that from the minima of the second derivative of the Landau functional Ω is shown by blue stars. The interaction dependence of the Kondo temperature T_K (black line with circles) and the temperatures $T_{c,\max}$ and $T_{c,\min}$ of the maxima and minima of the local charge compressibility $\chi_c(T)$ (blue dashed line with crosses and purple dashed line with triangles) are taken from Ref. [34]. The shaded area corresponds to the "plateau" of the temperature dependence of the effective local moment; see Ref. [34]. The critical interaction U_{c2} of the MIT taken from Ref. [36] is shown by the blue line; see text for the other notations. The inset zooms in on the region near the MIT.

Importantly, the temperature $T^*(U)$ of the appearance of quasiparticles, being close to the boundary of the plateau of the square of the effective local moment $T\chi_s(T)$ (χ_s is the local spin susceptibility; see Ref. [34]), is larger than the previously determined temperatures $T_{c,\min}$ of the minima of local charge compressibility, which mark the boundary of the screening of local magnetic moments [34]. This shows that quasiparticles appearing at $T^*(U)$ start to screen local magnetic moments at lower temperatures closer to $T_{c,\min}$. To see the trace of the screening of local moments on the temperature dependence of resistivity, we also show in the phase diagram the line of the exponents of resistivity $\beta = d\ln\rho/d\ln T = 1$, which is rather close to the $T_{c,\min}$ boundary. Therefore, the start of the screening of local magnetic moments is associated with the linear temperature dependence of the resistivity, which is inherited from the linear temperature dependence of the self-energy. This gives the possibility of experimental determination of the boundary of the beginning of the screening of local magnetic moments.

B. Away from half filling, $n < 1$

We first investigate the existence and screening of local magnetic moments away from half filling in a way similar to what was done at half filling in Ref. [34]. In Fig. 4 we show the temperature dependence of the square of the effective local magnetic moment $\mu^2_{\mathrm{eff}} = T\chi_s$ and the inverse static local spin susceptibility χ_s^{-1}, where $\chi_s = \int_0^\beta \langle s^z(\tau)s^z(0)\rangle$ and $s^z(\tau)$ is the local spin operator in the Heisenberg representation at the imaginary time τ. The inverse local susceptibility is almost linear in temperature, which shows the existence of LMMs in the low-temperature phase. Similar to what we did for half filling [34], we determine the Kondo temperatures T_K by fitting the obtained temperature dependences of $\mu_{\mathrm{eff}}(T)$ to the universal temperature dependence for the Kondo model [43,44]. We can see that the doping yields a reduction of the maximal effective local magnetic moment, which is reached at $T \sim 10T_K$. The plateau of the temperature dependence of μ^2_{eff}, which was obtained in the half-filled case [34], continuously disappears with doping, such that the Curie law $\chi_{\mathrm{loc}} \propto 1/T$ is not fulfilled in the intermediate-temperature range. At the same time, as mentioned above (see also the inset of Fig. 4), in a broad range of temperatures the inverse local spin susceptibility remains linear in temperature, fulfilling the Curie-Weiss law $\chi_{\mathrm{loc}} \propto 1/(T + T_W)$ with the Weiss temperature $T_W \approx \sqrt{2}T_K$, as suggested for the screened regime of the Kondo model [43–46]. In contrast to the half-filled case, this temperature dependence of the susceptibility is observed almost up to the maximum of the dependence $\mu_{\mathrm{eff}}(T)$. This shows that at finite doping the LMMs exist mainly in the screened regime.

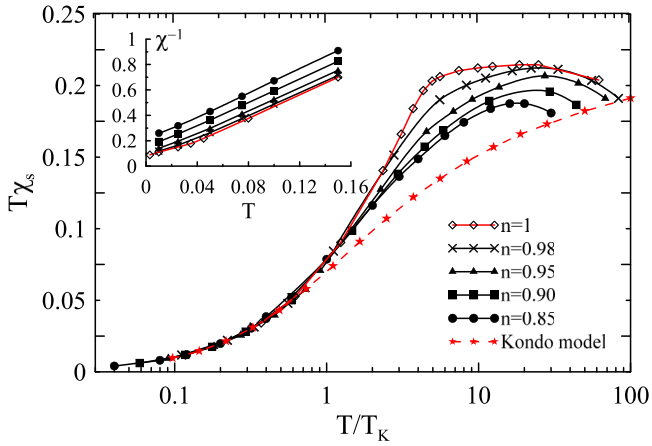

FIG. 4. Temperature dependence of the square of the effective local magnetic moment $\mu_{\rm eff}^2 = T\,\chi_s$ for different values of filling n and $U = 2.25$. The open rhombs correspond to $n = 1$, crosses correspond to $n = 0.98$, triangles correspond to $n = 0.95$, squares correspond to $n = 0.90$, and circles correspond to $n = 0.85$. The dashed line with stars shows the universal temperature dependence for the Kondo model [43,44]. The inset shows the temperature dependence of the inverse local spin susceptibilities.

The upper temperature boundary $T_{\rm SCR}$ of the regime of screening of local magnetic moments (which we denote in the following as SCR like for half filling) can be obtained from the minima of the temperature dependence of double occupation (see Fig. 5). In agreement with the discussion above, the corresponding temperatures are located somewhat below the maxima of the local magnetic moment $\mu_{\rm eff}(T)$. To understand the peculiarities of the SCR regime, we show in Fig. 6 the temperature dependence of local charge compressibilities $\chi_c(T) = dn/d\mu$, where the change in the chemical potential $d\mu$ acts only at the impurity site. For $n = 0.98$ and $n = 0.95$ we observe a behavior similar to that obtained at half filling [34] with the temperatures of the maxima of local compressibility $T_{c,\rm max}$ corresponding to the beginning of formation of local magnetic moments and the temperatures of minima of

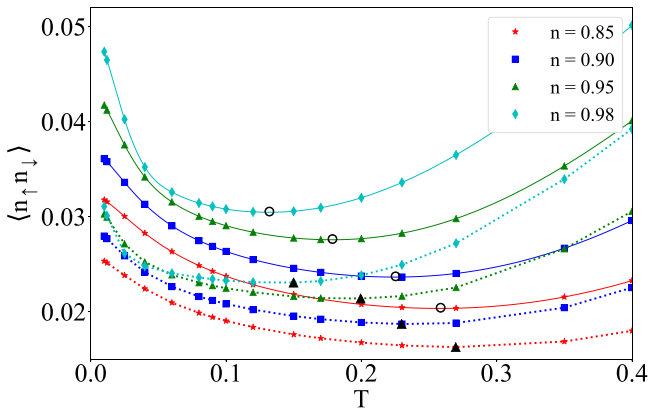

FIG. 5. Temperature dependence of the double occupation for different fillings n. Solid lines show data for $U = 2.25$; dotted lines are for $U = 2.5$. The black open circles (triangles) indicate minima of $\langle n_\uparrow n_\downarrow \rangle$ for $U = 2.25$ ($U = 2.5$).

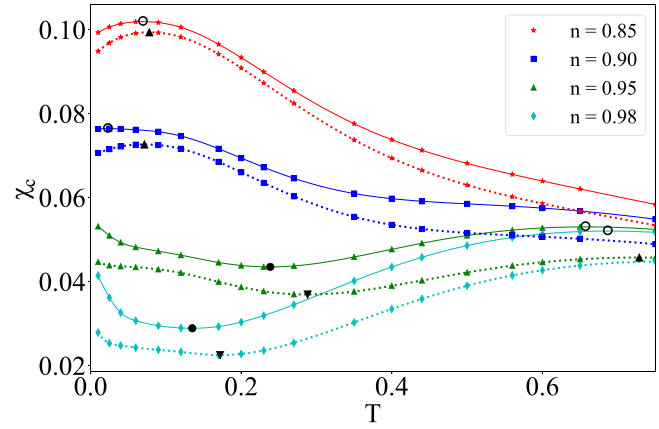

FIG. 6. Temperature dependence of the local static charge susceptibility χ_c at various fillings n. Solid lines show data for $U = 2.25$; dotted lines are for $U = 2.5$. The black solid circles (inverted triangles) indicate minima of χ_c for $U = 2.25$ ($U = 2.5$), the black opened circles (triangles) indicate maxima of χ_c for $U = 2.25$ ($U = 2.5$).

compressibility $T_{c,\rm min}$ corresponding to the beginning of the screening of LMMs. For these fillings, which are close to half filling, the minimum of charge compressibility appears to be close to that of double occupation, such that the two criteria of the screening of LMMs agree with each other (cf. Ref. [34]).

At the same time, for $n < 0.95$ the maximum of the local charge compressibility shifts to the much lower temperature $T_{c,\rm max} \sim 0.1$ deep inside the SCR regime, and the local minimum of compressibility is not observed. Physically, this appears due to a sufficiently large number of free coherent charge carriers. Accordingly, these carriers substantially contribute to the local charge compressibility, changing its temperature dependence, which can be interpreted as the delocalization of hole motion. Nevertheless, the local magnetic moments persist (although in the screened regime) even in this case, which can be seen from the above-discussed temperature dependences of static local spin susceptibility, as well as from the frequency dependences of the dynamic local spin susceptibilities $\chi_s(\omega)$. Indeed, the dynamic susceptibilities show a sharp peak at $\omega = 0$ (see Fig. 7), which is characteristic of the presence of LMMs [47,48]. In contrast to the half-filled case [34] the width of the peak increases with the decrease of temperature, which shows that the local moments' lifetime decreases. Also, the width of the peak increases with doping. However, the half-width of the peak $\Delta\omega \sim 0.03$–0.05 remains smaller than the temperature of the crossover to the SCR regime, which implies that the local moments in a substantial part of the SCR regime remain well defined.

Let us discuss how the temperature dependence of the resistivity changes with the decrease of the filling n. In Fig. 8(a) we show the temperature evolution of the resistivity for $U = 2.25$ (corresponding to the metallic phase at half filling) and $U = 2.5$ (corresponding to the insulating phase at half filling). As in the case of half filling and similar to results in previous studies of the doped Hubbard model on an infinite-dimensional hypercubic [22] and Bethe [27] lattices, close to half filling, there is a maximum of the resistivity at a certain temperature $T^*(U, n)$, which increases with the decrease of n.

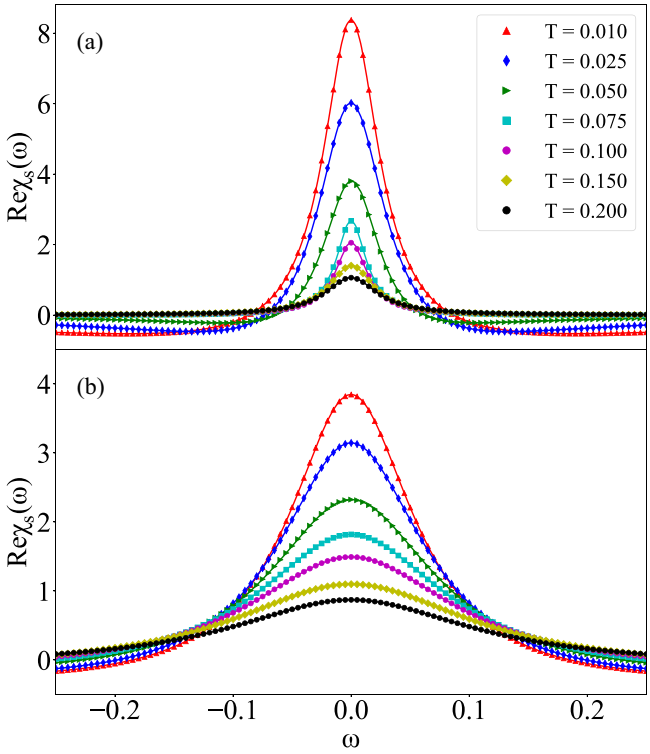

FIG. 7. Real frequency dependence of the real part of the local spin susceptibility $\chi_s(\omega)$ for $U = 2.25$ and (a) $n = 0.98$ and (b) $n = 0.85$.

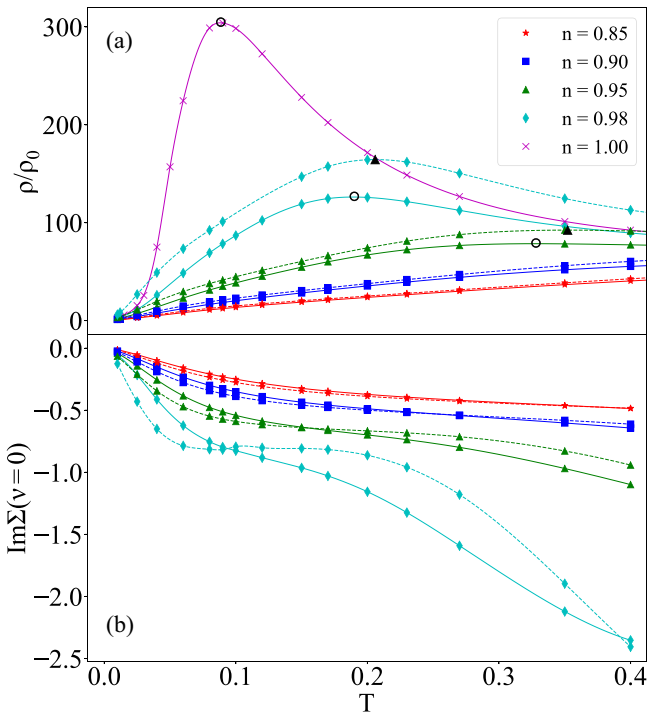

FIG. 8. Temperature dependences of (a) the resistivity [in units of $\rho_0 = \hbar/(4e^2)$] and (b) the imaginary part of the zero-frequency self-energy for various fillings n. Solid lines correspond to $U = 2.25$; dotted lines are for $U = 2.5$. The black open circles (triangles) indicate maxima of ρ for $U = 2.25$ ($U = 2.5$).

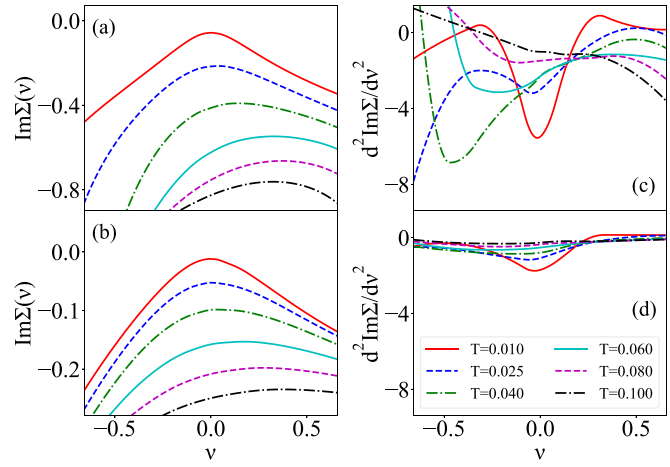

FIG. 9. The frequency dependences of (a) and (b) the imaginary part of the self-energy and (c) and (d) its second derivative for $U = 2.25$ and filling $n = 0.98$ (top) and $n = 0.85$ (bottom).

Suppression of the resistivity in comparison to the half filling $n = 1$ is related to smaller damping of the quasiparticles away from half filling (see below). The peak of the resistivity also becomes less pronounced, from which it can be assumed that the boundary between coherent and incoherent quasiparticle regimes becomes even less defined than for half filling. At the same time, the region of almost linear behavior of resistivity becomes broader than for $n = 1$, as obtained previously in Ref. [22] for the infinite-dimensional hypercubic lattice and in Ref. [36] for the square and triangular lattices.

The linear temperature dependence of the resistivity originates from the temperature dependence of the imaginary part of the self-energy [Fig. 8(b)], which shows almost linear behavior $\Gamma \simeq AT$ (with a small zero-frequency temperature-independent part) in the temperature range $T < 0.05$ and more complex behavior at higher temperatures; as mentioned above, the quasiparticle damping remains smaller than for $n = 1$ and decreases with a decrease in filling. The frequency dependence of the self-energy is shown in Fig. 9. In contrast to the half-filled case, we observe quasiparticle behavior for all considered temperatures. With a decrease of filling the second derivative of the self-energy with respect to frequency also decreases, which implies frequency behavior of the self-energy closer to linear.

Similar to half filling, the temperatures of the maxima $T^*(U, n)$ are located somewhat above the temperatures of the onset of screening T_{SCR}. To emphasize the origin of the maximum of the temperature dependence of resistivity at $n < 1$, in Fig. 10 we show the temperature evolution of the spectral functions for $n = 0.98$. We can see that the form of the spectral functions changes with an increase in temperature from having a central quasiparticle peak at the Fermi level at low temperatures, similar to that observed at half filling [34], to the monotonously decreasing density of states near the Fermi level, located at the upper edge of the lower Hubbard band. This behavior is similar to that for the particle-hole asymmetric Anderson impurity model [49,50]. The high-temperature form of the spectral functions (referred to below as the PLM+H regime) physically corresponds to

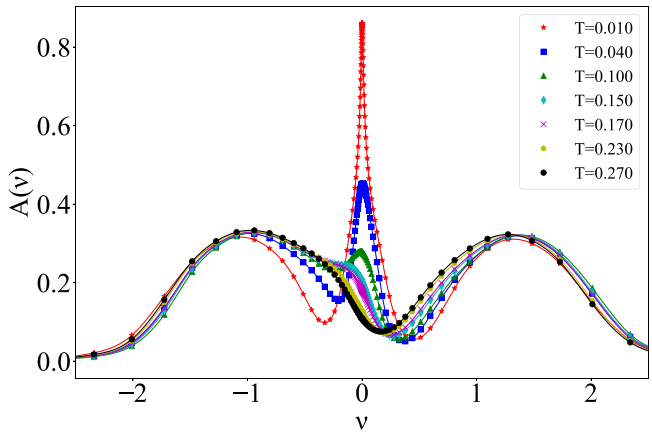

FIG. 10. The frequency dependences of the spectral function for $U = 2.25$, filling $n = 0.98$, and various temperatures T. The temperature range $T > 0.17$ is associated with the PLM+H regime, where the central quasiparticle peak is absent and the holes move incoherently in the background of local magnetic moments. The SCR regime ($T < 0.1$) is characterized by the narrow quasiparticle peak at the Fermi level.

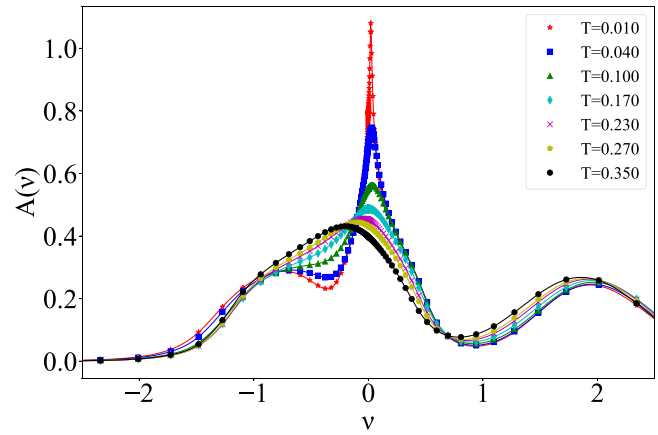

FIG. 11. The same as Fig. 10 for $n = 0.85$. The SCR regime ($T < 0.23$) is characterized by the narrow quasiparticle peak at the Fermi level.

holes, which move incoherently in the background of local magnetic moments. At the same time, the quasiparticle peak at low temperatures corresponds to the many-particle screening state. Near half filling (i.e., for $n = 0.98$) the temperature of the appearance of the quasiparticle peak, determined by the appearance of the inflection points of the energy dependence of the density of states near the Fermi level, is close to the temperature T^* at which the maximum of the resistivity is observed; the temperature T^* also coincides with reaching a maximal value of the local magnetic moment (see Fig. 4). Therefore, in this regime we associate the maximum of the resistivity with the crossover from the incoherent motion of holes to the presence of coherent quasiparticles.

Importantly, the crossover with the appearance of the quasiparticle peak at the Fermi level with lowering temperature occurs at all considered fillings $n \geqslant 0.85$, while the Fermi level shifts from the upper edge to the center of the lower Hubbard subband with the increase of the doping to $\delta = 1 - n \sim 0.15$ (see Fig. 11). In the latter case the Fermi level is far below the interaction-induced minimum of the local density of states, and as discussed above, the LMMs exist only in the screened state at low temperatures. On the other hand, the high-temperature form of the spectral function corresponds to coherently moving holes, referred to below as the CMH regime. The transition between the PLM+H and CMH regimes corresponds to the changing temperature dependence of the local charge susceptibility, discussed above for Fig. 6.

As mentioned above, at low temperatures an almost linear temperature dependence of the quasiparticle damping and resistivity occurs, which is reminiscent of the marginal Fermi liquid in Ref. [51]. We can therefore interpret this state as occurring due to competition of two effects: an increase of the coherence of quasiparticles due to the presence of a sufficient number of charge carriers and their decoherence due to the interaction with local magnetic moments. We note that a similar linear temperature dependence of the resistivity was previously obtained in the doped Kondo lattice model [52] and a compactified version of the single-impurity Anderson model [53].

The obtained results for $n < 1$ are collected in the phase diagram in Fig. 12. Close to half filling the temperature of the maximum of the resistivity, which determines the boundary of the PLM+H regime and the regime with present coherent

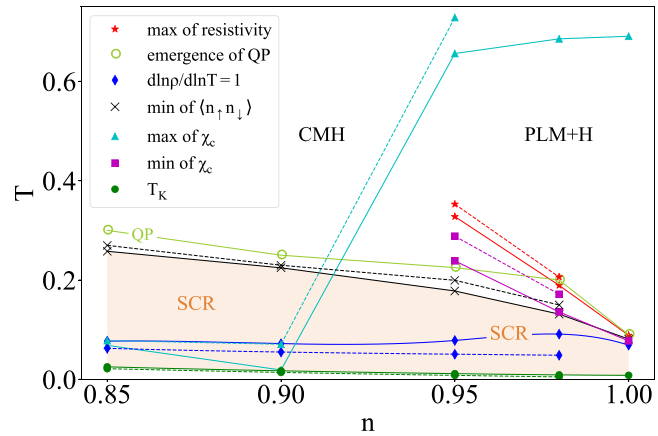

FIG. 12. The phase diagram away from half filling. Solid lines show data for $U = 2.25$; dotted lines are for $U = 2.5$. The turquoise line (triangles) shows maxima of $\chi_c(T)$, corresponding to the upper temperature boundary of the unscreened LMMs, and the purple line (squares) corresponds to minima of $\chi_c(T)$, which mark the beginning of the screening of LMMs in the PLM+H regime. The green line with open circles shows the appearance of a sharp quasiparticle peak (corresponding to the crossover to the QP regime). The black lines with crosses show minima of double occupation $\langle n_\uparrow n_\downarrow \rangle$, which bound the screening SCR regime (shaded orange area for $U = 2.25$); the Kondo temperatures are shown by green lines (circles). The red lines (stars) indicate maxima of $\rho(T)$, corresponding to the crossover from incoherent to coherent quasiparticle motion, and the blue lines (rhombs) show $\beta \equiv d \ln \rho / d \ln T = 1$ points, which mark the onset of the linear temperature dependence of quasiparticle damping and resistivity. For the form of the spectral functions in different regimes see Figs. 10 and 11.

quasiparticles, is somewhat larger than the temperatures of the minimum of double occupation and charge compressibility, which mark the onset of the screening regime $T_{\rm SCR}$. As described above, the screening of local magnetic moments in this regime is similar to that at half filling. With moving further away from half filling, the temperature of the onset of quasiparticles approaches the boundary of the SCR regime, which shows again that the local magnetic moments in this regime exist in the screened phase. In the interval of fillings $0.90 < n < 0.95$ the temperature of the local compressibility maximum sharply changes towards low temperatures, which, as we noted earlier, indicates delocalization of the charge carriers (i.e., holes). This idea is also supported by the fact that far away from half filling the resistivity $\rho(T)$ becomes monotonously increasing with temperature, which shows a different nature of fermionic quasiparticles close to and far away from half filling, corresponding to the crossover from the PLM+H to CMH regime.

The upper temperature boundary of the SCR regime, determined from the minimum of double occupation, increases only moderately with a decrease in n. As mentioned above, close to half filling this boundary is close to $T_{c,\min}$. At low temperatures $T \lesssim T_{\beta=1}$, where $T_{\beta=1} \sim 0.1$ is the temperature, at which the exponent $\beta \equiv d \ln \rho / d \ln T = 1$, we find almost linear behavior of the quasiparticle damping and the resistivity, which, as mentioned above, resembles the marginal Fermi liquid state. With the increase of the doping, the linear behavior of the resistivity becomes more pronounced.

IV. CONCLUSIONS

In the present paper we have considered the effect of local magnetic moments on the temperature dependence of resistivity. We have shown that the maximum of the temperature dependence of the resistivity $T^*(U, n)$, obtained with DMFT, corresponds to the beginning of the formation of the quasiparticle peak of the spectral function. Physically, the temperature $T^*(U, 1)$ marks the crossover from insulating to coherent quasiparticle behavior at half filling, while away from half filling $T^*(U, n)$ marks the crossover from incoherent to coherent motion of charge carriers and it is obtained only sufficiently close to half filling ($n \geqslant 0.95$).

At half filling, we considered the boundary for the appearance of quasiparticles, which in this case coincides with with the temperature of the maximum of the resistivity and is also close to the Widom line. An important aspect is that the appearance of quasiparticles does not necessarily cause screening of LMMs; the latter begins only after the coherence of quasiparticles with decreasing temperature becomes sufficient. The boundary of the beginning of the screening regime, previously defined by the minima of the local charge susceptibility and double occupation, perfectly corresponds to the exponent of the resistivity $\beta \equiv d \ln \rho / d \ln T = 1$.

Close to half filling we found that at not too low temperatures the local magnetic moments exist, together with incoherently moving holes. This is the regime described by the t-J model [16,54–56]; the present study shows, however, that it is restricted to only a few percent of doping. With lowering temperature, the LMMs are screened by itinerant electrons, similar to half filling. With moving further away from half filling, the hole motion becomes more coherent. In this case the LMMs exist only in the screened phase at sufficiently low temperatures, where the sharp quasiparticle peak of the spectral function emerges. The presence of both LMMs and coherent quasiparticles at sufficient doping yields, at low temperatures, a linear dependent scattering rate and resistivity below the temperature at which the exponent $\beta = 1$ is reached.

We therefore emphasize the complexity of the obtained physical properties of the doped phase, which, on the one hand, show features of conventional quasiparticle behavior at sufficient doping but, on the other hand, show traces of screened LMMs. While at high temperatures the crossover from the incoherent to coherent motion of holes is obtained, at low temperatures we find the SCR phase, whose properties are distinctly different from the coherent hole motion. This phase shows linear temperature dependence of the scattering rate and resistivity, reminiscent of a marginal Fermi liquid [51]. The appearance of incoherent holes at low doping, the onset of their coherence at larger doping $\delta \sim 0.1$, and the "marginal" Fermi liquid behavior at low temperatures highlight some similarities with the physics of high-temperature superconductors (see, e.g., Ref. [16]). For the description of these compounds, however, magnetic and, possibly, charge correlations likely have to be taken into account.

The inclusion of magnetic and/or charge correlations, e.g., within the dynamical cluster approximation (DCA) or cellular dynamical mean-field theory (CDMFT) approach, and/or nonlocal diagrammatic extensions of DMFT [57] is therefore of certain interest for future research. Another interesting topic is studying the effect of Hund's exchange in multiorbital models and considering the difference of "Mottness" and "Hundness" behavior of local magnetic moments.

Note added. Recently, we learned about a related study on the half-filled Hubbard model on a square lattice [58] which confirms the coincidence of the Widom line $T_{\rm QWL}(U)$ with the temperatures of the appearance of quasiparticles and the maximum of the resistivity, as well as onset of the screening of the local magnetic moments at lower temperatures, $T \leqslant T_{\rm SCR} < T_{\rm QWL}$.

ACKNOWLEDGMENTS

The authors acknowledge the financial support from the BASIS foundation (Grant No. 21-1-1-9-1) and the Ministry of Science and Higher Education of the Russian Federation (Agreement No. 075-15-2021-606). A.A.K. also acknowledges the financial support within the theme "Quant" AAAA-A18-118020190095-4 of the Ministry of Science and Higher Education of the Russian Federation.

[1] N. F. Mott, Proc. Phys. Soc. A **62**, 416 (1949).

[2] D. B. McWhan, T. M. Rice, and J. P. Remeika, Phys. Rev. Lett. **23**, 1384 (1969); D. B. McWhan and T. M. Rice, *ibid.* **22**, 887 (1969); D. B. McWhan, J. P. Remeika, J. P. Maita, H. Okinaka, K. Kosuge, and S. Kachi, Phys. Rev. B **7**, 326 (1973).

[3] M. Rubinstein, Phys. Rev. B **2**, 4731 (1970).

[4] D. B. McWhan, A. Menth, J. P. Remeika, W. F. Brinkman, and T. M. Rice, Phys. Rev. B **7**, 1920 (1973).

[5] K. Held, G. Keller, V. Eyert, D. Vollhardt, and V. I. Anisimov, Phys. Rev. Lett. **86**, 5345 (2001); G. Keller, K. Held, V. Eyert, D. Vollhardt, and V. I. Anisimov, Phys. Rev. B **70**, 205116 (2004); D. Vollhardt, K. Held, G. Keller, R. Bulla, Th. Pruschke, I. A. Nekrasov, and V. I. Anisimov, J. Phys. Soc. Jpn. **74**, 136 (2005).

[6] V. I. Anisimov, D. E. Kondakov, A. V. Kozhevnikov, I. A. Nekrasov, Z. V. Pchelkina, J. W. Allen, S.-K. Mo, H.-D. Kim, P. Metcalf, S. Suga, A. Sekiyama, G. Keller, I. Leonov, X. Ren, and D. Vollhardt, Phys. Rev. B **71**, 125119 (2005).

[7] A. I. Poteryaev, J. M. Tomczak, S. Biermann, A. Georges, A. I. Lichtenstein, A. N. Rubtsov, T. Saha-Dasgupta, and O. K. Andersen, Phys. Rev. B **76**, 085127 (2007).

[8] P. Hansmann, A. Toschi, G. Sangiovanni, T. Saha-Dasgupta, S. Lupi, M. Marsi, and K. Held, Phys. Status Solidi B **250**, 1251 (2013).

[9] Y. Kurosaki, Y. Shimizu, K. Miyagawa, K. Kanoda, and G. Saito, Phys. Rev. Lett. **95**, 177001 (2005).

[10] T. Furukawa, K. Miyagawa, H. Taniguchi, R. Kato, and K. Kanoda, Nat. Phys. **11**, 221 (2015).

[11] A. Pustogow, M. Bories, A. Löhle, R. Rösslhuber, E. Zhukova, B. Gorshunov, S. Tomić, J. A. Schlueter, R. Hübner, T. Hiramatsu, Y. Yoshida, G. Saito, R. Kato, T.-H. Lee, V. Dobrosavljević, S. Fratini, and M. Dressel, Nat. Mater. **17**, 773 (2018).

[12] W. Li, A. Pustogow, R. Kato, and M. Dressel, Phys. Rev. B **99**, 115137 (2019).

[13] A. Pustogow, Y. Saito, A. Löhle, M. S. Alonso, A. Kawamoto, V. Dobrosavljević, M. Dressel, and S. Fratini, Nat. Commun. **12**, 1571 (2021).

[14] Y. Saito, A. Löhle, A. Kawamoto, A. Pustogow, and M. Dressel, Crystals **11**, 817 (2021).

[15] A. Pustogow, R. Rösslhuber, Y. Tan, E. Uykur, A. Böhme, M. Wenzel, Y. Saito, A. Löhle, R. Hübner, A. Kawamoto, J. A. Schlueter, V. Dobrosavljević, and M. Dressel, npj Quantum Mater. **6**, 9 (2021).

[16] P. A. Lee, N. Nagaosa, and X.-G. Wen, Rev. Mod. Phys. **78**, 17 (2006).

[17] J. Spalek, J. Solid State Chem. **88**, 70 (1990).

[18] Ph. Noziéres, J. Phys. Soc. Jpn. **74**, 4 (2005).

[19] M. Fabrizio, in *The Physics of Correlated Insulators, Metals, and Superconductors*, edited by E. Pavarini, E. Koch, R. Scalettar, and R. M. Martin, Lecture Notes of the Autumn School on Correlated Electrons, Modeling and Simulation, Vol. 7 (Verlag des Forschungszentrum Jülich, Jülich, Germany, 2017), Chap. 13.

[20] A. Georges, G. Kotliar, W. Krauth, and M. Rozenberg, Rev. Mod. Phys. **68**, 13 (1996); G. Kotliar and D. Vollhardt, Phys. Today **57**(3), 53 (2004).

[21] Th. Pruschke, D. L. Cox, and M. Jarrell, Phys. Rev. B **47**, 3553 (1993).

[22] M. Jarrell and Th. Pruschke, Phys. Rev. B **49**, 1458 (1994); Th. Pruschke, M. Jarrell, and J. K. Freericks, Adv. Phys. **44**, 187 (1995).

[23] J. Merino and R. H. McKenzie, Phys. Rev. B **61**, 7996 (2000).

[24] M. M. Radonjić, D. Tanasković, V. Dobrosavljević, K. Haule, and G. Kotliar, Phys. Rev. B **85**, 085133 (2012).

[25] H. Terletska, J. Vučičević, D. Tanasković, and V. Dobrosavljević, Phys. Rev. Lett. **107**, 026401 (2011).

[26] J. Vučičević, H. Terletska, D. Tanasković, and V. Dobrosavljević, Phys. Rev. B **88**, 075143 (2013).

[27] J. Vučičević, D. Tanasković, M. J. Rozenberg, and V. Dobrosavljević, Phys. Rev. Lett. **114**, 246402 (2015).

[28] H. Eisenlohr, Seung-Sup B. Lee, and M. Vojta, Phys. Rev. B **100**, 155152 (2019).

[29] A. Reymbaut, M. Boulay, L. Fratino, P. Sémon, W. Wu, G. Sordi, and A. M. S. Tremblay, arXiv:2004.02302.

[30] B. Widom, in *Phase Transitions and Critical Phenomena*, edited by C. Domb and M. S. Green, Vol. 2 (Academic Press, New York, 1972), Chap. 3.

[31] G. G. Simeoni, T. Bryk, F. A. Gorelli, M. Krisch, G. Ruocco, M. Santoro, and T. Scopigno, Nat. Phys. **6**, 503 (2010).

[32] P. Chalupa, T. Schäfer, M. Reitner, D. Springer, S. Andergassen, and A. Toschi, Phys. Rev. Lett. **126**, 056403 (2021).

[33] E. A. Stepanov, S. Brener, V. Harkov, M. I. Katsnelson, and A. I. Lichtenstein, Phys. Rev. B **105**, 155151 (2022).

[34] T. B. Mazitov and A. A. Katanin, Phys. Rev. B **105**, L081111 (2022).

[35] E. G. C. P. van Loon, F. Krien, and A. A. Katanin, Phys. Rev. Lett. **125**, 136402 (2020).

[36] A. Vranić, J. Vučičević, J. Kokalj, J. Skolimowski, R. Žitko, J. Mravlje, and D. Tanasković, Phys. Rev. B **102**, 115142 (2020).

[37] R. Žitko and T. Pruschke, Phys. Rev. B **79**, 085106 (2009).

[38] O. Parcollet, M. Ferrero, T. Ayral, H. Hafermann, I. Krivenko, L. Messio, and P. Seth, Comput. Phys. Commun. **196**, 398 (2015); https://triqs.github.io/nrgljubljana_interface/.

[39] M. Jarrell and Th. Pruschke, Z. Phys. B **90**, 187 (1993).

[40] T.-F. Fang, N.-H. Tong, Z. Cao, Q.-F. Sun, and H.-G. Luo, Phys. Rev. B **92**, 155129 (2015).

[41] L. Huang, Y. Wang, Z. Y. Meng, L. Du, P. Werner, and X. Dai, Comput. Phys. Commun. **195**, 140 (2015); L. Huang, *ibid.* **221**, 423 (2017).

[42] A. S. Belozerov, A. A. Katanin, and V. I. Anisimov, arXiv:2206.12383.

[43] K. Wilson, Rev. Mod. Phys. **47**, 773 (1975).

[44] H. R. Krishna-murthy, J. W. Wilkins, and K. G. Wilson, Phys. Rev. B **21**, 1003 (1980).

[45] V. I. Mel'nikov, JETP Lett. **35**, 511 (1982).

[46] A. M. Tsvelick and P. B. Wiegmann, Adv. Phys. **32**, 453 (1983).

[47] A. A. Katanin, A. I. Poteryaev, A. V. Efremov, A. O. Shorikov, S. L. Skornyakov, M. A. Korotin, and V. I. Anisimov, Phys. Rev. B **81**, 045117 (2010).

[48] P. A. Igoshev, A. V. Efremov, A. I. Poteryaev, A. A. Katanin, and V. I. Anisimov, Phys. Rev. B **88**, 155120 (2013).

[49] B. Horvatić, D. Šokčević, and V. Zlatić, Phys. Rev. B **36**, 675 (1987).

[50] A. C. Hewson, *The Kondo Problem to Heavy Fermions* (Cambridge University Press, Cambridge, 1993).

[51] C. M. Varma, P. B. Littlewood, S. Schmitt-Rink, and E. Abrahams, and A. E. Ruckenstein, Phys. Rev. Lett. **63**, 1996 (1989).

[52] M. Lavagna, C. Lacroix, and M. Cyrot, J. Phys. F **12**, 745 (1982).

[53] G.-M. Zhang and A. C. Hewson, Phys. Rev. Lett. **76**, 2137 (1996).

[54] C. Castellani, C. Di Castro, D. Feinberg, and J. Ranninger, Phys. Rev. Lett. **43**, 1957 (1979).
[55] J. E. Hirsch, Phys. Rev. Lett. **54**, 1317 (1985).
[56] M. Cyrot, Solid State Commun. **60**, 253 (1986).
[57] G. Rohringer, H. Hafermann, A. Toschi, A. A. Katanin, A. E. Antipov, M. I. Katsnelson, A. I. Lichtenstein, A. N. Rubtsov, and K. Held, Rev. Mod. Phys. **90**, 025003 (2018).
[58] Z. Long, J. Wang, and Y.-F. Yang, Phys. Rev. B **106**, 195128 (2022).